energies

Article

Earthquake Algorithm-Based Voltage Referenced MPPT Implementation through a Standardized Validation Frame

Alexandro Ortiz [1,*], Efrain Mendez [1,2], Israel Macias [1] and Arturo Molina [3]

1 School of Engineering and Sciences, Tecnologico de Monterrey, Mexico City 14380, Mexico
2 Department of Mechanical and Aerospace Engineering, University of California, Irvine, CA 92617, USA
3 Institute of Advanced Materials for Sustainable Manufacturing, Tecnologico de Monterrey, Mexico City 14380, Mexico
* Correspondence: alexandro.ortiz@tec.mx; Tel.: +52-811-499-6196

Abstract: This paper presents a new direct maximum power point tracking (MPPT) with a reference voltage (V_{ref}) based on the metaheuristic earthquake algorithm (EA) where the optimization variable is the V_{ref} for hard-switching converters. The efficiency and performance of EA-MPPT-V_{ref} is compared with the perturb-and-observe (P&O) counterpart technique due to the fact that it is widely used for commercial products. Static and dynamic responses for both MPPT strategies are evaluated, which correspond to steady-state oscillations when they are near the maximum power point (MPP), and the tracking-speed, respectively. The efficiency was evaluated with the EN 50530 standard. The results show that the new MPPT proposed is a competitive method using the EA to obtain the optimal voltage reference. From static results, EA-MPPT VP presented a better efficiency of 5.13% and 3.23% for European and California energy commission (CEC) efficiency, respectively. Whereas, from dynamic results, MPPT-V_{ref} techniques presented an efficiency from 95.13% to 99.91%, and 99.01% to 99.91% of the total power of the PV system for P&O and EA strategies, respectively.

Keywords: MPPT; FPGA; DC-DC converter

check for updates

Citation: Ortiz, A.; Mendez, E.; Macias, I.; Molina, A. Earthquake Algorithm-Based Voltage Referenced MPPT Implementation through a Standardized Validation Frame. *Energies* **2022**, *15*, 8971. https://doi.org/10.3390/en15238971

Academic Editor: Mario Marchesoni

Received: 11 October 2022
Accepted: 24 November 2022
Published: 27 November 2022

1. Introduction

Since 1995, global energy demand has been increasing by 53% (according to the average annual growth rate of just 1.87∼2.1% of total energy supply and consumption). This high demand has generated a depletion of fuel resources, which supply about 80% of total energy consumed [1]. On the other hand, the use of fossil fuels deteriorates air quality, contributing to the global warming effects. For this reason, renewable energies have been adopted to reduce the use of fossil fuels to decrease carbon emissions [2].

Therefore, renewable energy has become more necessary than ever to discover the alternative of energy to supply the total energy demand. Between all renewable energies such as wind, geothermal, hydro, solar and biomass power, solar power is the most common for electricity generation, e.g., electric vehicles stations, energy storage systems, streetlights, heating equipment, home electricity, renewable energy hybrid system, etc. [3].

Generally, photovoltaic (PV) cells are the most used technology to convert solar energy into electricity due to advantages such as low maintenance cost, no fuel consumption (zero carbon emission), no moving parts and self-generated noise, and that they can be installed in many places. However, the limitations of PV system include low conversion efficiency and the searching for the maximum power point (MPP), determined by the surrounding environment [4,5]. To deal with the difficulties resulting from low-efficiency conversion, strategies have been developed to obtain the maximum power from PV systems. There are two main ways to track the solar energy: (1) mechanical, where the sun position is tracked, and (2) electrical, where the maximum point of voltage and current is searched for; this strategy is known as maximum power point tracking (MPPT) [6]. To find the MPP of PV systems is difficult due to its non-linear voltage-current (V-I) characteristic curve which can be modified by solar irradiance, ambient temperature, wind speed and other environment parameters [7]. Therefore, to operate in the MPP of the PV system, it is necessary to insert a converter direct current-direct current (DC/DC) or direct current-alternating current (DC/AC) between the PV and electric load. The MPPT algorithm must be embedded into the converter in order to continuously adapt the input load impedance of the PV system to track the instantaneous MPP [8].

According to [9], there are two main categories of MPPT techniques: (1) direct, and (2) indirect. Direct methods can work without any knowledge of PV system characteristics. By sensing the voltage and current of the PV system, it is possible to track the MPP. Sampling and modulation techniques are two kinds of direct control strategy. In sampling techniques, voltage and current are collected and compared with the present and past values in order to locate the MPP, while in modulation techniques, automatic oscillations are generated as a feedback signal to find the MPP. On the other hand, the indirect methods employ numerical estimation using technical data from the PV array and parameter values. Thus, they cannot precisely track the MPP of PV array at any irradiance and cell temperature of PV system given [10]. Similar classifications are presented in [10,11] where MPPT methods are classified into three groups: (1) conventional and direct control techniques, (2) indirect control methods, and (3) soft computing-based approaches. In [5], identical classification is presented: (1) conventional methods, (2) intelligent techniques, and (3) nature-inspired or metaheuristic algorithms.

Based on conventional/direct methods, the perturb and observe (P&O) technique is the most used due to its easy structure and implementation; several recent implementations and improvements are presented in the following studies [12–22]. This algorithm presents the following behaviors: first, the PV voltage is perturbed; then, the power of PV system is observed to compare with the previous one. If the power increases, it means that the operating point has moved toward the MPP, and the perturbation must be continued in the same direction. Otherwise, if the power from PV system decreases, the perturbation must be changed and reversed due the operating point moving away from the MPP. Nevertheless, the disadvantages of this method are: (1) when is near of the MPP presents steady-state oscillations, (2) poor efficiency in cloudy days, and (3) slow response to rapid changes in weather conditions. Another direct technique is the incremental conductance (IC) presented by [23–29] in recent years. This algorithm is based on the incremental (dI/dV) and instantaneous conductance (I/V) of the PV system in order to detect the slope of the power-voltage (P-V) curve. If the incremental is equal to the negative instantaneous conductance, it means that the algorithm reaches the MPP. On the other hand, if the incremental conductance is greater or less than instantaneous, the operating point is at the left and right side of the MPP, respectively. The main weakness of this algorithm is the uncertainties due to the noise of components and when the solar irradiation increases. For the fractional open-circuit voltage (FOCV) method [30,31], it is based on the relationship between the open-circuit voltage (V_{oc}) and the voltage at maximum power (V_{mp}) of the PV system. Commonly, a constant K_{pv} is presented which is the voltage factor with the value in the range 0.7–0.9. The V_{oc} is measured periodically disconnecting the load; then, the V_{mp} is estimated using the K_{pv} which is typically specified in the panel's datasheet. However, the frequency and duration to estimate the V_{mp} can be improved when it is high, but the power loss is increased.

Regarding the MPPT intelligent/indirect methods, the most used techniques (in recent years) for MPPTs are fuzzy-logic (FL) [32–51] controller, artificial neural networks (ANN) [52–60], and Kalman Filter (KF) [61]. In FL, the model of the system is not necessary and this is an important advantage due to the non-linearities and uncertainties presented in a model. Therefore, steady state and dynamical performance is improved by FL. However, the qualitative reaction of the system to different inputs must be prior known by the designer. Moreover, these implementation methods present lack for adaptivity with various operating points of PV systems [50]. On the other hand, ANN provides accurate and robust PV modeling and can deal with uncertain weather conditions if it is well trained. With these considerations, ANN provides a very fast and precise MPPT to locate and track the MPP. Nevertheless, the main drawback is that the ANN needs to be trained recurrently due to time/temperature variations of the PV arrays characteristics. Thus, the ANN accuracy depends on the ANN being comprehensively trained [62]. According to KF, this method applies two steps: (1) prediction and (2) correction. For MPPT application, the first step of KF is estimate the V_{mp}. The second step is to correct the estimation by calculating the error between the PV voltage measured and the estimated V_{mp}. This process is iterative until the error is close to 0. However, the main disadvantage is that KF uses the slope of P-V curve, and it is impossible to estimate the global MPP (GMPP) [11]. Moreover, implementation of these techniques in large-scale PV systems generates difficulties on the control system when it is implemented. Furthermore, the implementation of these techniques is very complex and demands high-level experience of user [63].

In [64], metaheuristic optimization algorithms supply a better switching between finding an approximate optimal solution and convergence speed using less hardware resources. Besides, these algorithms adopt strategies developed from artificial intelligence (AI), operation research, and soft-computing, which empower the optimization strategies that are convenient for conventional or high complex optimization problems [65]. According to [66], metaheuristic optimization algorithms provide a better trade-off. Moreover, [67] highlights that metaheuristic algorithms have been implemented to improve the performance to track the MPP in PV system. This can be useful to reduce the sensitivity of the algorithm to these parameters that do not allow reaching the global optimum or the solution stuck in a local optimum. Several metaheuristic MPPT methods are presented in the last year, such as particle swarm optimization (PSO) [68–77], genetic algorithm (GA) [78–82], differential evolution (DE) [27,83,84], cuckoo search optimization (CSO) [4,85,86], ant colony optimization (ACO) [87–89], firefly algorithm (FA) [90,91], chaotic search (CS) [92], artificial bee colony (ABC) [93], grey wolf optimizer (GWO) [94], bat algorithm (BA) [95], shuffled frog-leaping algorithm (SFLA) [96], monkey king evolution (MKE) [97], salp swarm algorithm (SSA) [98], remora optimization algorithm (ROA) [67], and EA [99]. Generally speaking, MPPT metaheuristic approach algorithms show improvement in tracking speed, tracking accuracy, and robustness. In addition, the speed of convergence and tracking accuracy can be improved by providing compensation using the exploration and exploitation features of metaheuristic algorithms. Furthermore, these algorithms do not need any pre-set configuration and can be applied directly to any PV system without having information about its characteristics. However, the main drawback of these algorithms is their higher probability of falling into a local optimum in the tracking process which results in the inability to reach the global peak. Figure 1 shows the chronology of the MPPT studies carried out in recent years, where metaheuristic algorithms were used in most cases.

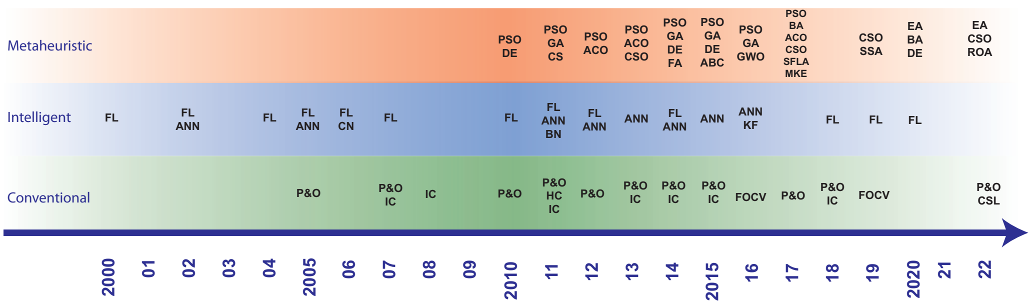

Figure 1. Timeline of different MPPT techniques in recent years.

Therefore, this work presents an MPPT strategy based on the EA metaheuristic optimization algorithm presented in [100]. In addition, to improve performance, a proportional-integral (PI) controller is integrated. First, the EA-MPPT estimates the optimal voltage that provides the maximum power of the photovoltaic system. Then, the optimum voltage is sent to a PI controller as a reference voltage (V_{ref}) which modifies the duty cycle of the DC/DC converter to achieve this voltage. Besides, in order to compare the efficiency of the proposed EA-MPPT, the P&O-MPPT strategy are implemented due that is the most MPPT used in commercial products with the IC algorithm, according to [11]. Aditionally, when P&O and IC are evaluated with EN50530 standard test, results indicate similar performance [17,18].

Another key factor to consider from the literature review is that many MPPT algorithms have been proposed with different techniques and strategies in order to improve the accuracy and performance of static and dynamic response. In addition, in some studies, different strategies of different classifications have been combined to hybridize the behavior between them. In these works, authors compared the MPPT algorithms using step changes in the irradiance or temperature of the PV systems. These steps are not standardized and it is difficult to compare their performance objectively [8]. Hence, in this work, the proposed EA-MPPT algorithm is evaluated with the standard test EN 50530 which is composed of two tests: static and dynamic. This test evaluates the efficiency of the MPPT algorithms analyzing the dynamic response which correspond to the performance of the tracking speed and the static response which is determined by the steady-state oscillations when they are near of the MPP. Moreover, the standard test EN 50530 evaluates the MPPT efficiency according to real-world weather conditions from different regions such as: (1) middle-Europe climate [101] and (2) US south-west regions [102].

The main contribution of this paper can be summarized as follows:

- A new MPPT based on EA algorithm is proposed with an improvement that integrates a PI controller.
- We evaluate the proposed EA-MPPT strategy with the EN 50530 standard test that uses real-world weather conditions.
- We implement the proposed EA-MPPT embedded into a LabVIEW-FPGA frame in order to explore computational parallelism and compare it with the P&O counterpart.

This paper is organized as follows: Section 2 explains the P&O-MPPT strategy with reference voltage, then Section 3 presents the proposed voltage reference-based MPPT based on EA. Additionally, Section 4 describes the experimental setup and Section 5 depicts the EN 50530 test to evaluate the efficiency of MPPT strategies in static and dynamic responses. Finally, Section 6 presents the results and Section 7 concludes this work.

2. Voltage Reference Based MPPT

Conventional MPPT methods are widely used due their simplicity to implement, low computational cost, and unnecessary prior knowledge of the PV system. However, these methods present disadvantages, such as the amount of perturbation which may produce lost energy when they are near of the MPP (by steady-state oscillations) or decrease tracking speed (by a small perturb step) when they are in the search of the MPP [11]. Furthermore, their performance decreases when a rapid change in irradiance occurs [62]. Therefore, variable or adaptive perturbance has been proposed to improve the performance and generate a good trade-off between faster response and steady-state oscillations [103]. Furthermore, P&O could not determine when the MPP is actually reached [104].

Figure 2a presents the basic topology for MPPT controller which is connected directly to the DC/DC converter. In this case, the duty cycle for pulse-width modulation (PWM) signal is adjusted by the MPPT controller. In contrast, Figure 2b shows the voltage-based MPPT method which estimates the voltage reference to be compared with the measured PV voltage. Then, the result of the comparison is used as an error signal to the PI controller which adjusts the duty cycle in order to find the MPP from PV system. It is important to mention that only the DC/DC converter is presented but it can be combined with more power electronic components to create specific power electronic devices such as inverters.

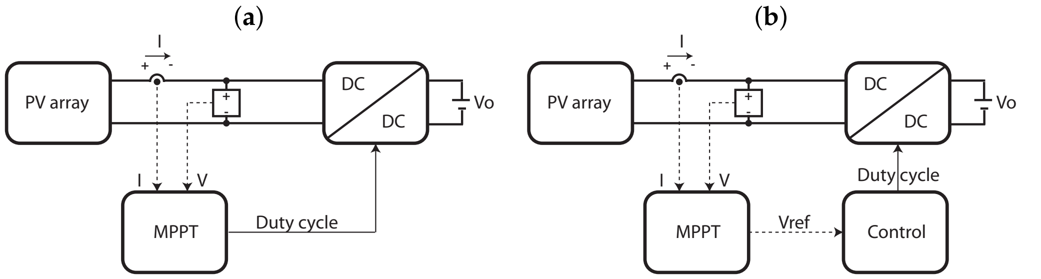

Figure 2. (**a**) General topology for conventional MPPT and (**b**) general topology for voltage reference-based MPPT.

Voltage Reference Based P&O MPPT Method

The P&O technique is the most well-liked MPPT method due to its simple structure. Therefore, hardware implementation is easy and has low computational cost. This technique is an iterative approach, and each iteration perturbs the PV voltage system (V_{pv}), and the output power is compared with the previous one. If the power is increasing, the perturbation will continue, otherwise perturbation is reversed. These perturbations can be defined as a small variation of duty cycle which generates changes in the response of the PV system. The use of large or small step-size increases the power oscillations (which will result in loss energy) or decelerates the tracking speed, respectively, [8]. Another aspect to be considered is the sampling rate, which also contributes to the performance of MPPT [105]. In [106], it is suggested that the sampling rate should be selected by the dynamic response of the DC/DC converter.

According to [107], the issues mentioned above can be improved by implementing a reference voltage (V_{ref}) control. In this case, the MPPT algorithm estimate the disturbance signal (V_{ref}) to send through the PI controller as an input reference which regulates the manipulation variable (duty cycle) for the DC/DC converter. Moreover, Figure 3 depicts the flowchart of P&O based on V_{ref}. The strategy is similar to the original P&O, where voltage and current of PV system is measured to estimate the present power and compare it with the previous one. Then, the present PV voltage is compared with the last voltage to make a decision which consists of increasing or decreasing the V_{ref}. The V_{ref} is the input reference to the PI controller in order to update the manipulation variable (duty cycle) to change the PV voltage with the DC/DC controller.

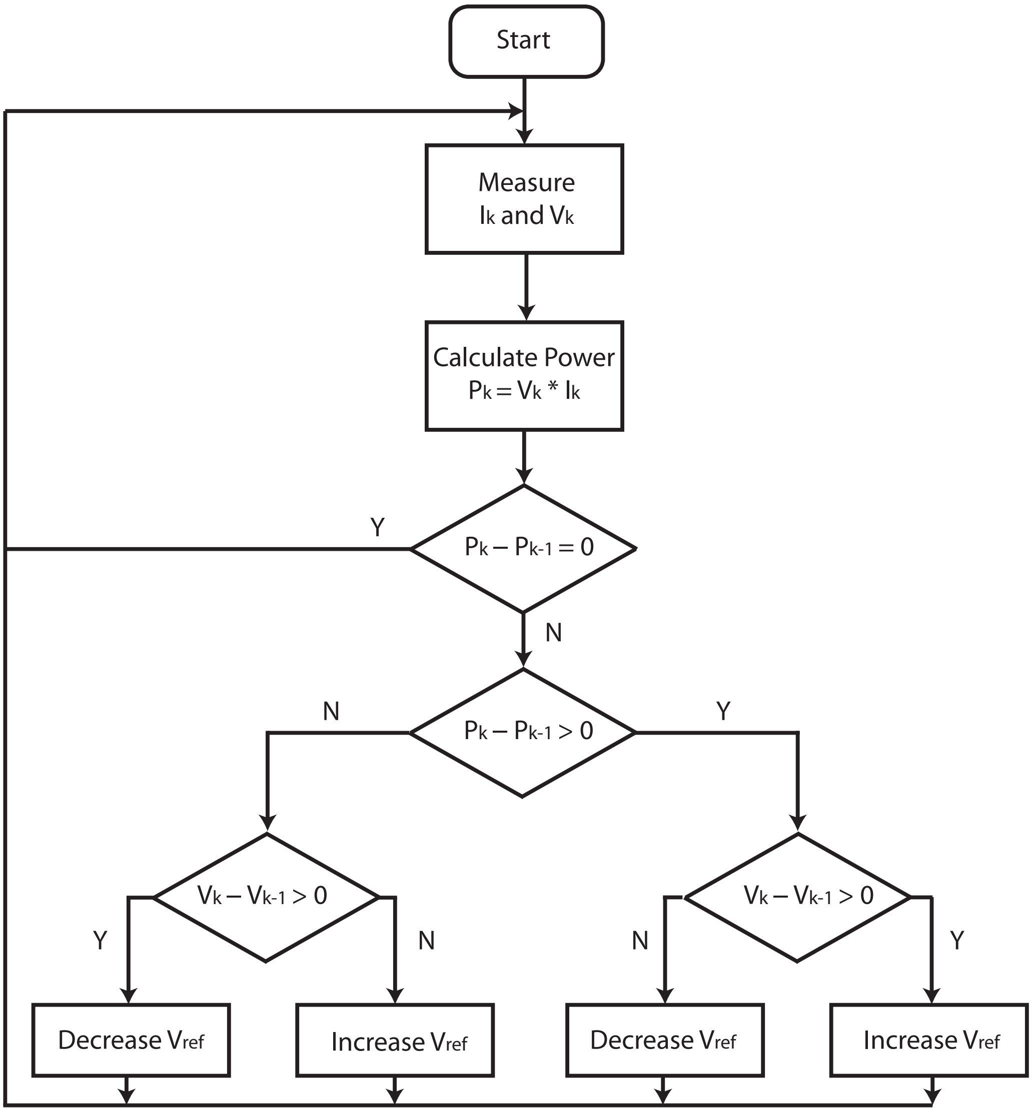

Figure 3. Flowchart of P&O based on voltage referenced for MPPT.

3. MPPT-EA Reference Voltage

3.1. Overview of EA

The EA algorithm is widely presented and implemented in many applications and platforms (as reported in [65]). Moreover, it is the first geological metaheuristic algorithm inspired by the earthquake phenomenon. The nature of earthquake is composed of P and S waves which the P-wave occurs first due to its higher speed than S-wave [100].

The P-wave is transmitted by any medium (solid, gas, and liquid) causing compression and tension of the medium and their velocity depends on earth material compressibility. Thus, volume changes occur when these characteristics are presented (Figure 4a). On the other hand, the transmission of the S-wave depends on rock elasticity. Its movement causes epicenters which are moved up and down perpendicular to the wave propagation direction (Figure 4b) [108].

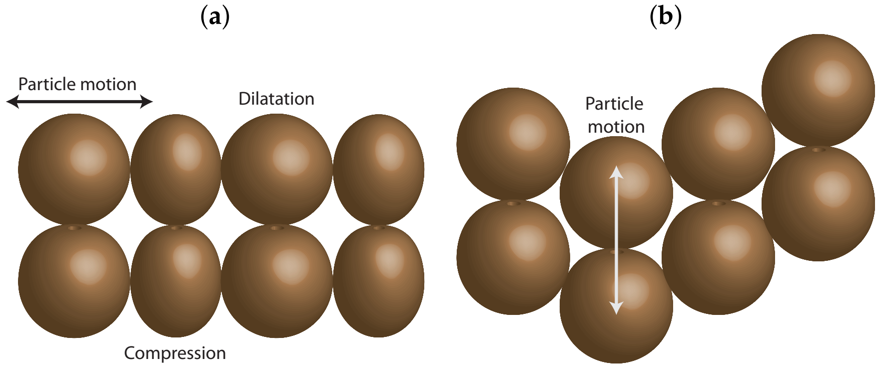

Figure 4. (**a**) P-wave and (**b**) S-wave from earthquake phenomenon.

Hence, mathematical estimation of P and S-wave is made in (1) and (2),

$$v_p = \sqrt{\frac{\lambda + 2\mu}{\rho}}, \tag{1}$$

$$v_s = \sqrt{\frac{\mu}{\rho}}, \tag{2}$$

where v_p and v_s are the P- and S-wave, respectively; λ and μ are the ground earth materials which are called Lamé parameters, and ρ is the density of the earth material (according to [100]). Furthermore, the selected values from Lamé parameters for optimal performance are $\lambda = \mu = 1.5$ GPa. Supplementary to the velocity's estimation, the densities of earth materials are taken from a random value in a range between 2200 and 3300 kg m^3 [65].

Considering the use of two different velocity equations in EA, in [100] introduces the concept of S-range (Sr) in order to define whether to use v_p or v_s. The Sr parameter defines the range situated near the global best epicenter (solution). Therefore, each epicenter uses v_p (exploration) or v_s (exploitation) to update its position depending on which zone (in or out of Sr range) is located previously.

3.2. Proposed EA-MPPT-V_{ref}

In [99], a first MPPT adaption based on EA metaheuristic optimization was presented. The authors extrapolated the dynamic optimization behavior from original EA to generate a MPP tracker with the EA feature. In simple terms, to find the MPP, it is necessary that the epicenters are moving around to provide a good optimal solution near the MPP. Hence, in order to ensure this dynamic, a searching flag (S_{flag}) was implemented to introduce the duty cycle (the one that collects the most power) to the searching positions, achieving a trade-off between tracking speed and steady-state oscillations when the MPP is reached. Another important aspect for this adaptation is the use of the v_s that is estimated with (2), to update the epicenter's position which is the reference voltage (V_{ref}).

Regarding what is proposed in this work, the MPPT-EA algorithm estimates the optimal voltage located in V_{mp} which, later, is the input for the PI controller as V_{ref}. The PI controller then modifies the duty cycle of the PWM signal which is the manipulation variable to eliminate any errors. Figure 5 depicts the flowchart of the proposed MPPT which estimates the V_{ref} with the behavior of EA algorithm that is adapted to PV system requirements. Then, this algortihm returns the best global epicenter (V_{ref}) after evaluating the epicenter and analyzing the response of the PV systems before exploring the next epicenter.

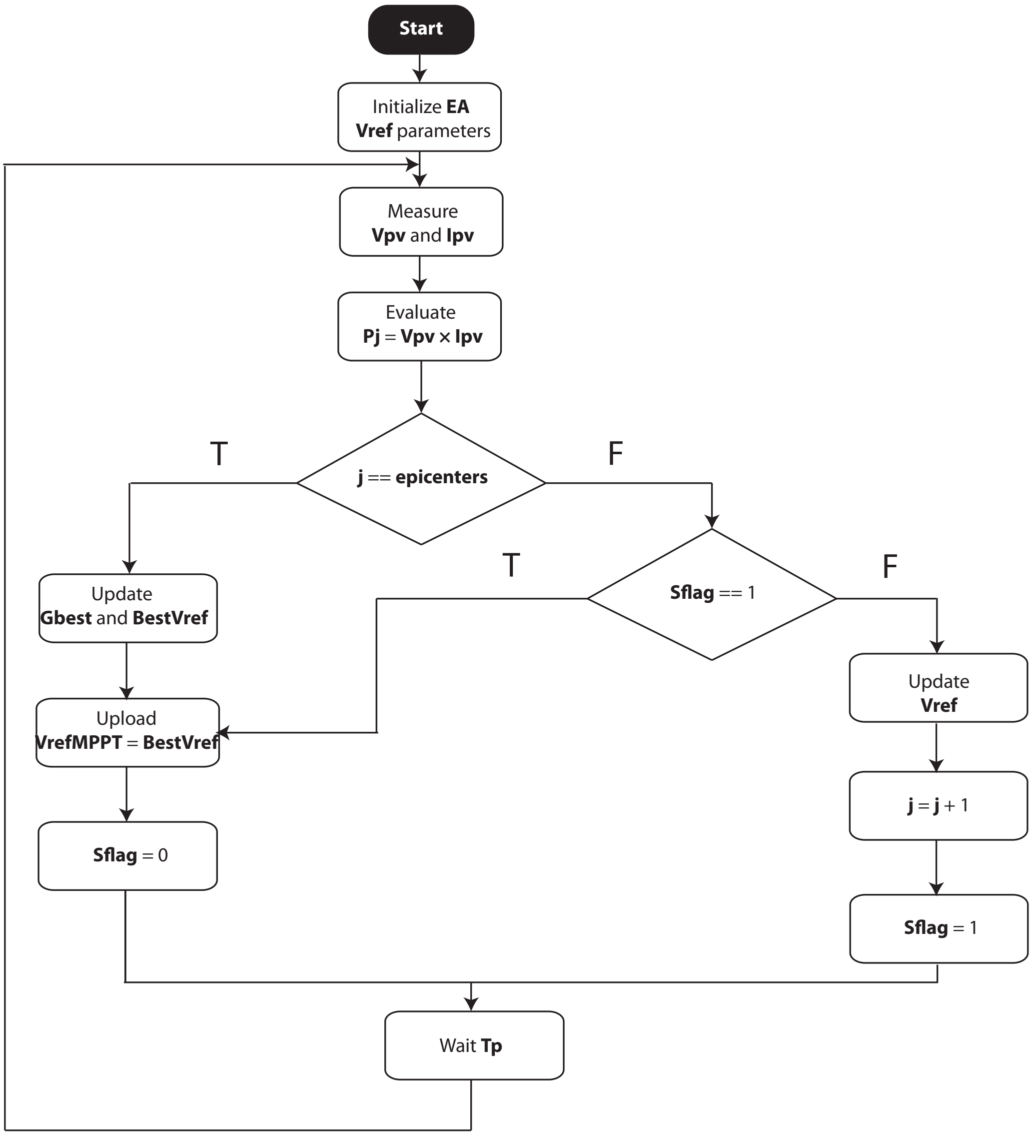

Figure 5. Flow chart of the Earthquake Algorithm-based Voltage Referenced MPPT.

4. Testbed System

The testbed system used for this work uses the platform for a request paten in [109]. This research facility was created to analyze energy consumption, storage, and generation patterns by conventional methods (i.e., fossil fuels) and renewable energies. Therefore, any energy consumption pattern can be reproduced and analyzed for distributed generation systems.

The experimental system for this work consists of four main blocks: (1) panel system, (2) DC/DC converter, (3) dynamic load, and (4) control and acquisition system. The PC host interacts with the acquisition and control systems, besides, sends virtual instrument software architecture (VISA) through standard commands for programmable instruments (SCPI) in order to change the parameterization of panel system (for the photovoltaic array simulator) and dynamic load. This interaction is achieved through a managed Ethernet switch which all devices are connected (as shown in Figure 6). The acquisition system captures five signals from the process system. The signals are: (1) voltage of the PV system, (2) current of the PV system, (3) voltage of load, (4) current of load, and (5) duty cycle. Moreover, the photovoltaic array simulator, when in the EN50530 test, storages the following data: (1) voltage at maximum power (V_{mp}), (2) current at maximum power (I_{mp}),

(3) maximum power (P_{mp}), (4) PV voltage, (5) PV current, (6) PV power, (7) measured energy, (8) MPP energy, and (9) MPPT efficiency.

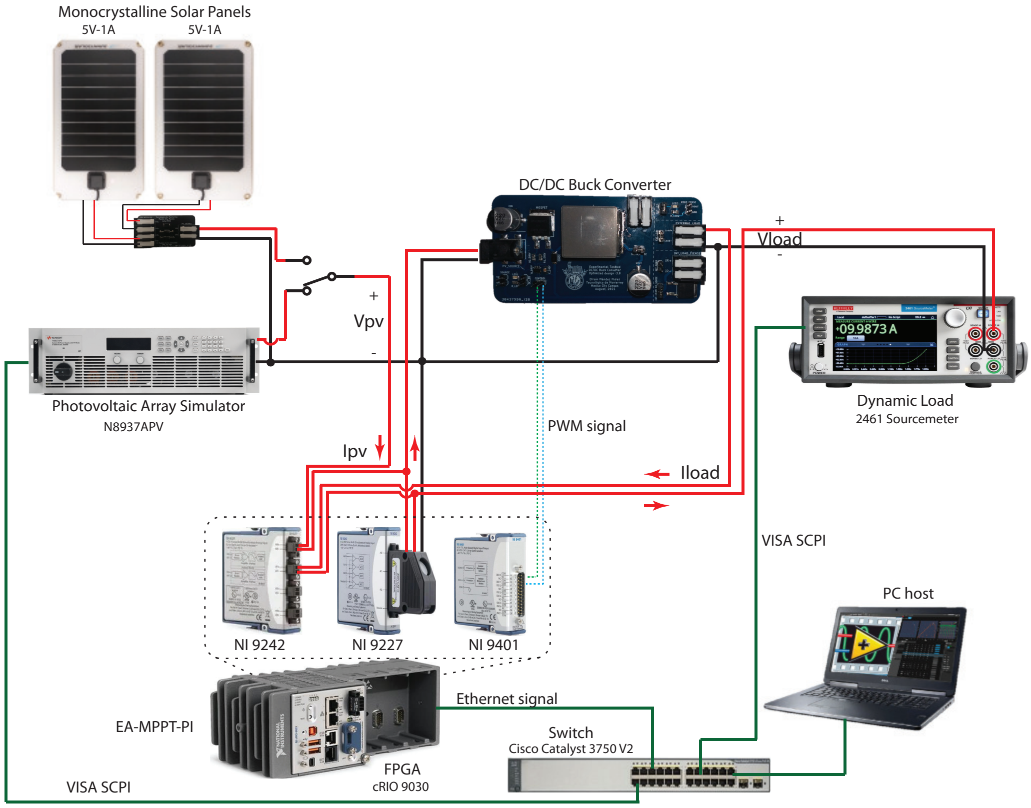

Figure 6. Testbed components interaction.

4.1. Solar Panel System

The experimental panel system is divided into two parts: (1) two monocrystalline solar panels and (2) photovoltaic array simulator. The monocrystalline solar panels consist of two-panel solar in series array of 5W each panel, with the following characteristics: open-circuit voltage (V_{oc}) = 6 V, short-circuit current (I_{sc}) = 1.1 A, voltage at max. power (V_{mp}) = 10 V, current at max power (I_{mp}) = 1 A, and maximum power (P_mp) = 10 W.

Figure 7 shows the implemented testbed to characterize the panel solar system. Four halogen lamps of 500 W each were used to emulate the solar irradiance. Moreover, a dynamic load was configured to sweep the load voltage to find the curves (I-V and P-V).

4.2. PV Array Simulator

To standardize the experiments, the photovoltaic array simulator (N8937APV, Keysight Technologies, Santa Rosa, CA, USA) was used to reproduce the output characteristics of a photovoltaic array allowing test maximum power point tracking (MPPT) algorithms and inverter efficiency (Figure 8). The photovoltaic array simulator has characterizations of photovoltaic panels with different standards such as: IEC60904, IEC61727, EN50530, and Sandia National Laboratories Photovoltaic Systems. Moreover, the software Keysight SAS control was used to manipulate the photovoltaic array simulator to evaluate the MPPT algorithms with the EN50530 dynamic and static test. In Section 5, the EN50530 standard test will be explained.

Figure 7. Solar panel experiment to obtain the V-I and V-P curves.

Figure 8. Photovoltaic array simulator N8937APV.

For this project, European Standard EN 50530 for solar array terrestrial model was selected to reproduce in the PV array simulator with the real characteristics from PV real system. This model is estimated by (3)–(5) and it can be found in [110]:

$$I_0 = I_{sc}(1 - \frac{I_{mp}}{I_{sc}})^{\frac{1}{1-\frac{V_{mp}}{V_{oc}}}}, \tag{3}$$

$$C_{aq} = \frac{\frac{V_{mp}}{V_{oc}} - 1}{\ln(1 - \frac{I_{mp}}{I_{sc}})}, \tag{4}$$

$$I = I_{sc} - I_0(e^{\frac{V}{V_{oc}C_{aq}}} - 1), \tag{5}$$

where I_0 and C_{aq} are parameters used for this model and V and I are the estimated voltage and current of the PV system model. I_{sc}, V_{oc}, V_{mp}, I_{mp} are parameters of the aforementioned characteristics of the PV system.

Figure 9a,b shows the comparison between the solar panel system (two monocrystalline solar panels) and the photovoltaic array simulator (PVsim).

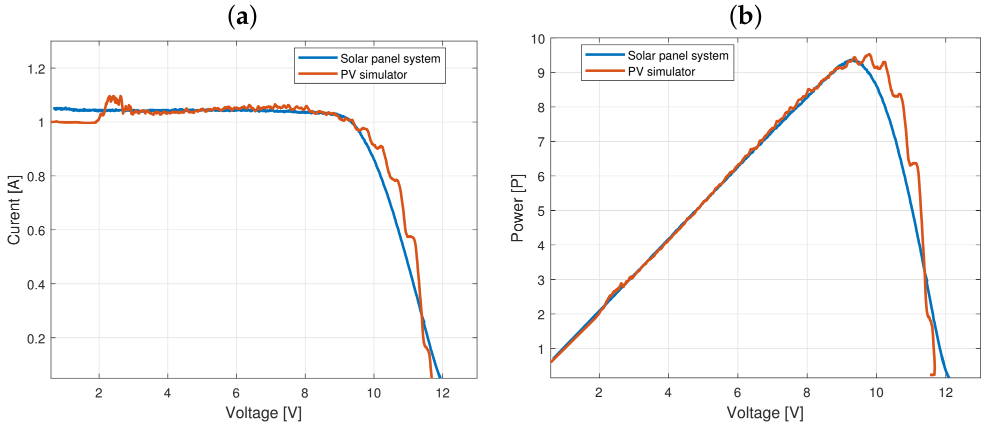

Figure 9. (**a**) V-I curve and (**b**) V-P curve.

Hence, Figure 10 presents the I-V and P-V curves from PVsim with different irradiances and temperatures.

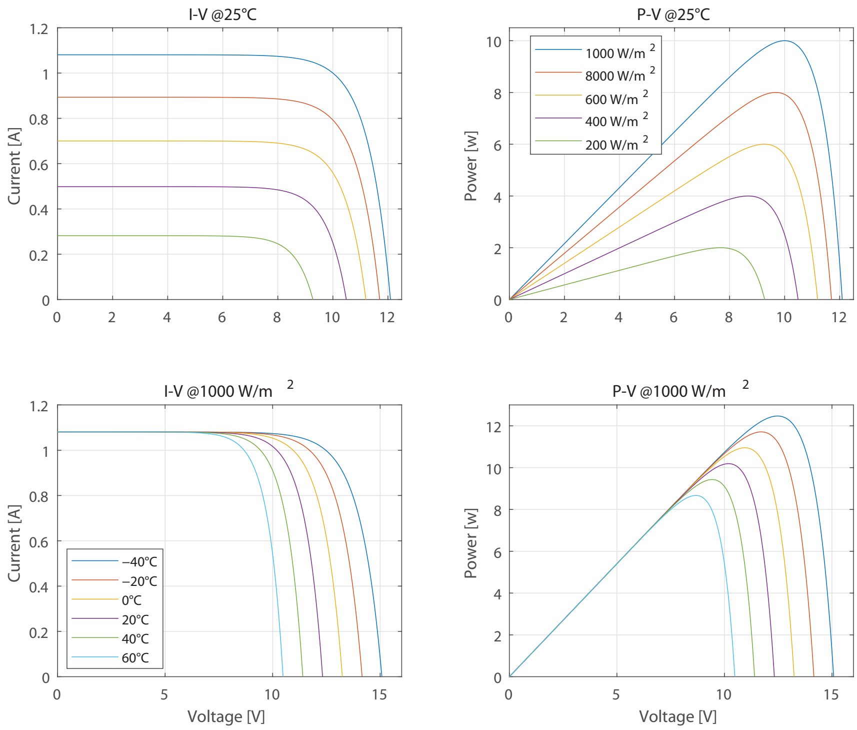

Figure 10. V-I and V-P curves representation of model from PVsim.

4.3. DC/DC Converter

For this work, a DC/DC buck converter was used to evaluate the V_{ref} MPPT. This buck converter was designed in [111] using EA optimization to generate a novel design methodology for inductance selection. The novel methodology and the implementable solution showed the feasibility of this approach. Moreover, the proposed solution reached the expected performance for fast voltage response with a low current slope with a low ripple inductor's voltage and current.

4.4. LabVIEW FPGA

To understand the results and the implementation limitations from V_{ref} MPPT-oriented study, it is important to emphasize the main features from the selected hardware for the embedded MPPT. Figure 11 depicts the main components of the cRIO-9030 hardware.

To exploit the parallel processing of FPGA, four loops were used (Figures 12–15): (1) PWM signal generation, (2) data acquisition and MPPT-V_{ref} execution, (3) PI controller for V_{ref}, and (4) sending data for data collection through FIFOs (First-In, First-Out).

Figure 11. cRIO-9030 LabVIEW FPGA features.

Figure 12 shows the while loop used for PWM signal generation. In this case, a signal generation function from LabVIEW FPGA features was used for the PWM signal. Then, the signal value was transformed into Boolean value to send into one Digital Output (DO) channel from NI 9401 digital module.

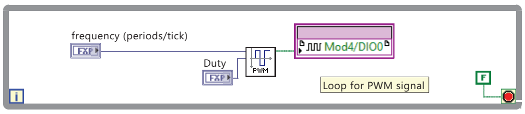

Figure 12. Loop for PWM signal creation.

Regarding data acquisition and MPPT-V_{ref} execution, NI 9242 module was used to read the current from PV array or PV simulator and DC/DC buck converter output. The NI 9227 module reads the voltage from PV array or PV simulator and DC/DC converter output. Both modules have 24-bit ADC resolution and 50 kS/s sampling rate. In addition, for each signal, root mean square (RMS) function was applied to send to the MPPT-V_{ref}. When the MPPT starts, all variables are initialized to start the estimation of the first V_{ref}. The estimation begins when RMS function sends a boolean signal that its process has finished and V_{ref} is estimated according to the MPPT algorithm flowchart (P&O and EA) as seen in Figure 13.

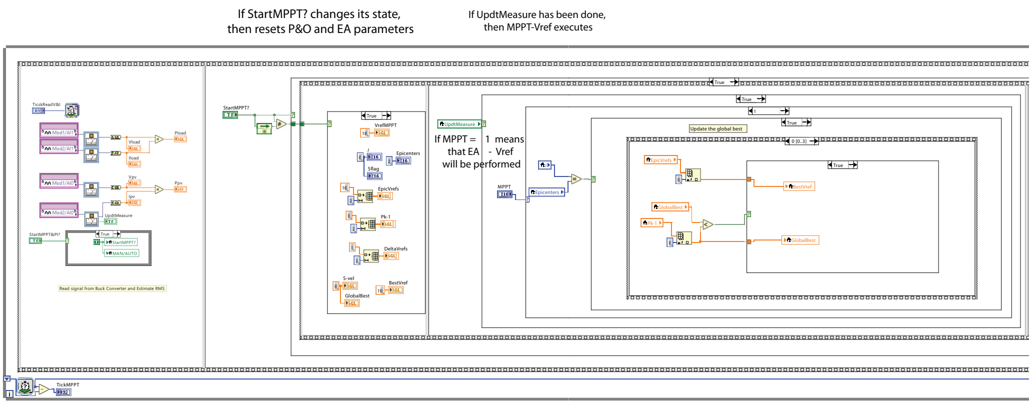

Figure 13. Loop for Data Acquisition and MPPT-V_{ref} execution.

Once the V_{ref} is estimated, the PI controller is responsible for rectifying the PV voltage with the V_{ref}. Figure 14 depicts the loop for control of referenced voltage. The duty cycle is estimated by the PI controller and send it to the loop for PWM signal generation.

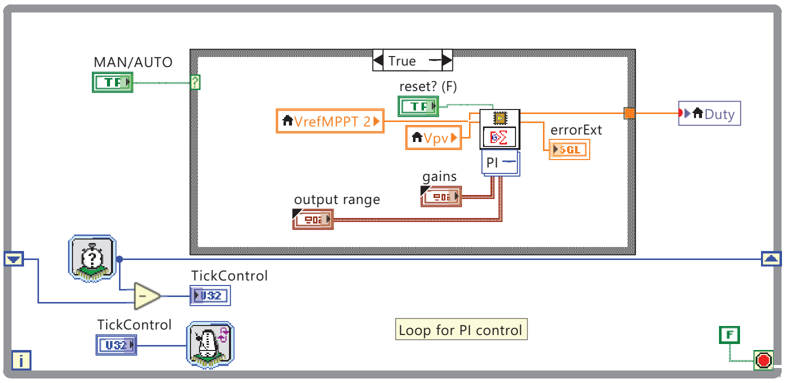

Figure 14. Loop for V_{ref} control.

Finally, a loop is necessary for sending data through FIFOs (LabVIEW FPGA) to the PC host in order to storage the following data: (1) PV voltage, (2) PV current, (3) load voltage, (4) load current, and (5) duty cycle.

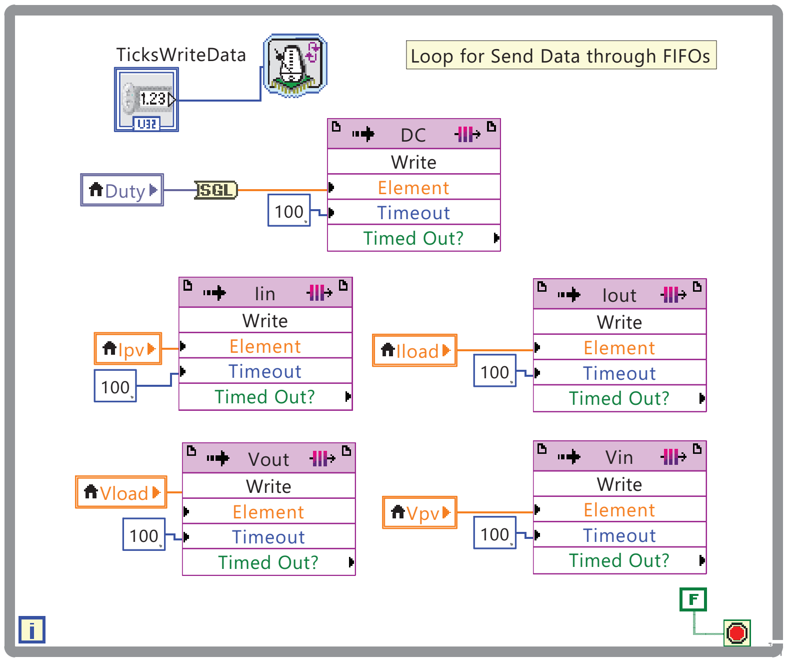

Figure 15. Loop for sending data through FIFOs.

5. EN50530 Test

To evaluate the performance of MPPT-V_{ref} algorithms, an EN 50530 test was performed using the PV simulator and Keysight SAS Control® software (Version 2021, Keysight Technologies, Santa Rosa, CA, USA). Figure 16 shows the interface for dynamic testing, which consists of 16 sub-tests with separate times of ramps and slopes; the total duration of the test is 6 h.

Regarding the static EN 50530 test, Figure 17 visualizes the interface where the current I-V and P-V curves and the present MPP is represented in a red circle. The total evaluation is composed of 24 sub-tests, which are divided by 3 MPP voltages: (1) 12.5 V, (2) 10 V, and (3) 8.4 V. These MPP voltages were selected according to the curves obtained in Figure 6, where irradiance is from 200 to 1000 W/m^2. The total duration of the static test is 6 h.

Figure 16. Keysight SAS Control Interface for Dynamic Test.

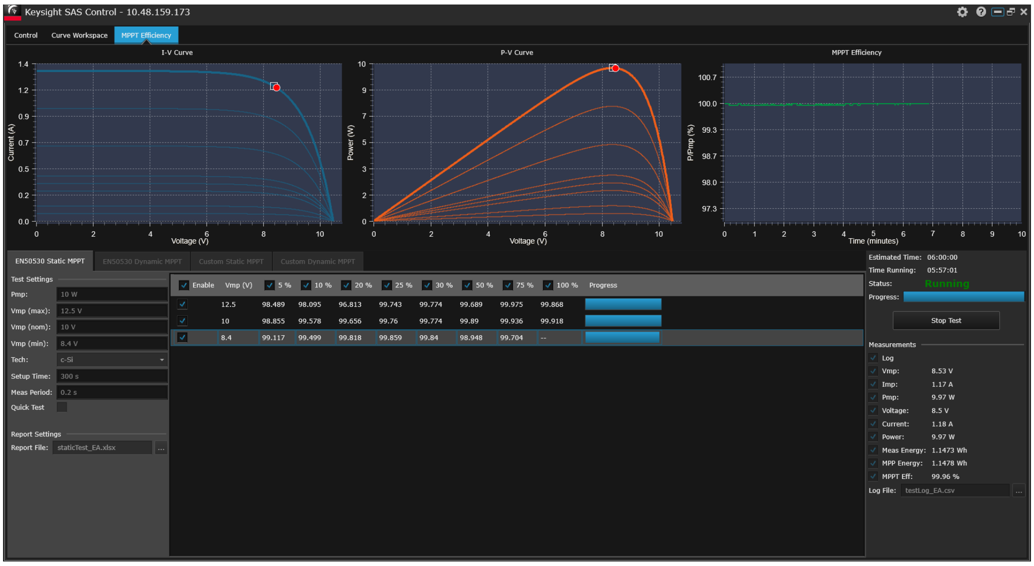

Figure 17. Keysight SAS Control Interface for Static Test.

5.1. Dynamic Test

Figures 18 and 19 depict the dynamic test for different ranges of irradiance. Each test starts with a waiting time of 300 s. After, a different number of ramps with dwell time of 10 s (up and down) and different slopes are defined as shown in Figure 18 where the irradiance range is from 100 to 500 W/m^2.

The second group for dynamic test is described by Figure 19, the irradiance range is from 300 to 1000 W/m^2. They have 10 ramps and dwell time is 10 s with different slopes.

Finally, Figure 20 depicts the last dynamic test, which is defined by one ramp with dwell time of 30 s, and slope of 0.1 W/m^2 per second.

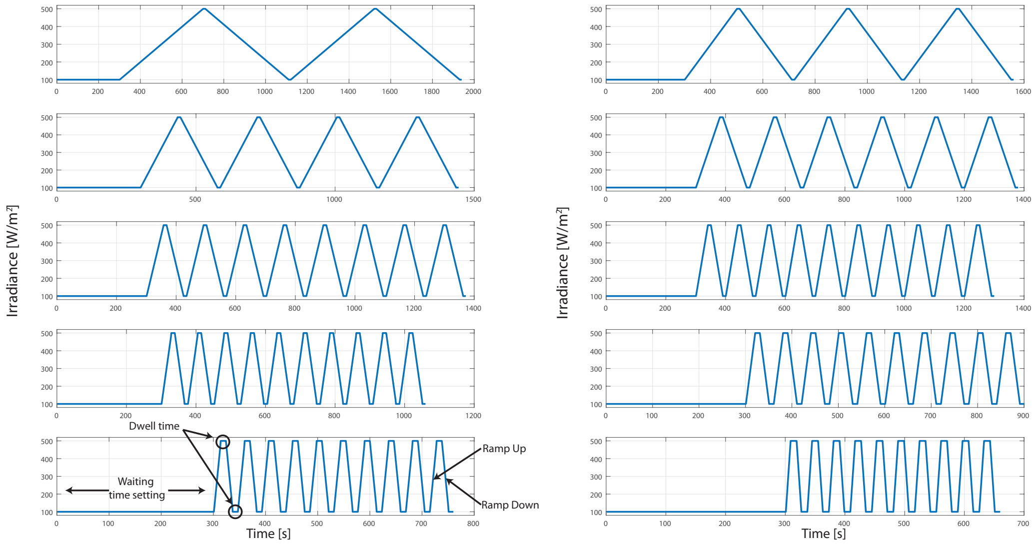

Figure 18. Dynamic test representation from 100 to 500 irradiance.

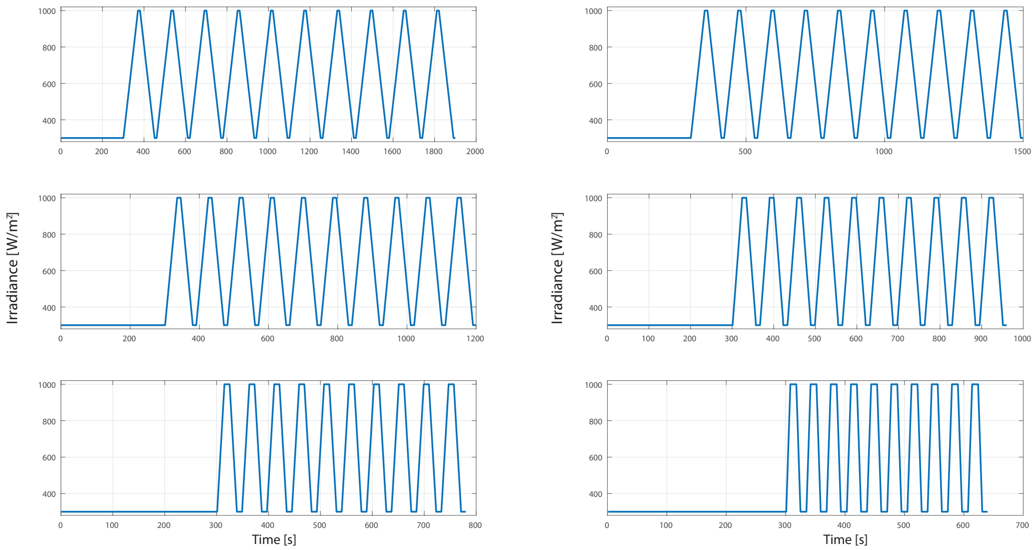

Figure 19. Dynamic test representation from 300 to 1000 irradiance.

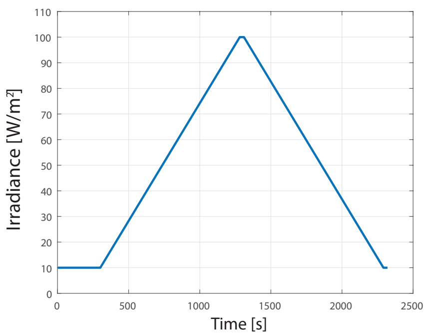

Figure 20. Dynamic test representation from 10 to 100 irradiance.

5.2. Static Test

From the static test, Table 1 shows the MPP voltages selected (12.5, 10.0 and 8.4 V) for every test. Each MPP voltage is evaluated at different irradiances: 5, 10, 20, 25, 30, 50, 75, and 100%; and each sub-test has a duration of 600 s, with a setup time of 300 s.

Table 1. Statistic test parameters.

MPP Voltage (V)	Irradiance (%)
12.5 10.0 8.4	5, 10, 20, 25, 30, 50, 75, 100

6. Results

To compare both MPPT-$Vref$ algorithms from EN 50530 standard test, Tables 2 and 3 present the MPPT efficiency for P&O and EA based on referenced voltage. In addition, Figures 21–23 present the density plot for P&O and EA MPPT-V_{ref} which represents the steady-state oscillations when the MPPT is near of the MPP.

Table 2. EN 50530 static test report.

MPPT Algorithm	MPP Voltage	Irradiance (%)								European Efficiency	CEC Efficiency
		5	10	20	25	30	50	75	100		
P&O	12.5	97.671	76.264	92.949	94.356	94.383	94.813	99.319	99.252	94.402	96.536
EA		98.489	98.095	96.813	99.743	99.774	99.689	99.975	99.868	99.249	99.652
P&O	10.0	91.469	77.385	75.210	81.177	97.992	99.392	98.901	97.325	94.452	96.771
EA		98.855	99.578	99.656	99.760	99.774	99.890	99.936	99.918	99.807	99.878
P&O	8.4	99.227	99.130	99.307	99.344	99.265	99.556	99.367	92.557	99.421	99.042
EA		99.117	99.499	99.812	99.859	99.840	98.948	99.704	99.962	99.340	99.572

6.1. Static Report

The static test evaluates the MPPT performance by measuring two efficiencies: European and CEC. The European efficiency is an averaged operating efficiency over a yearly power distribution corresponding to middle-Europe climate [101]. Meanwhile, CEC efficiency models the climates of higher isolations for US south-west regions, according to [102].

In the case of 12.5 V for MPP, EA-MPPT presents a better efficiency of 5.13% and 3.23% for European and CEC efficiency, respectively. For the MPP voltage of 10 V, EA-MPPT enhances the performance in 5.67% for European and 3.21% for CEC efficiency. Finally, in the specific case of 8.4 V for MPP, both efficiencies are similar (minor variations, <1%).

Density plots for 8.4 V_{mp} are shown in Figure 21 with the objective of showing the steady-state oscillations. From the results, the V_{ref} for each MPPT algorithm presents the following behavior: mean of 8.48 V and standard deviation of 0.1605 V and mean of 8.74 V and standard deviation of 0.1860, for EA and P&O, respectively.

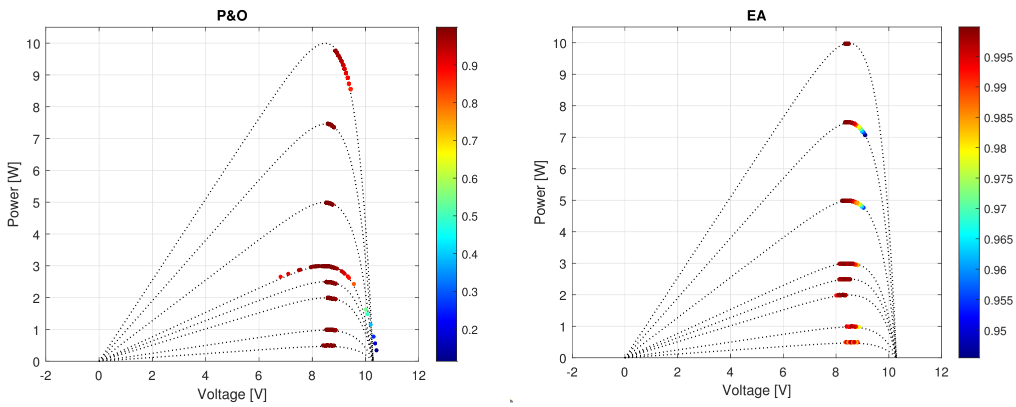

Figure 21. MPPTs behavior in static tests at V_{mp} = 8.4 V.

At V_{mp} of 10 V, steady-state oscillations at low irradiances are more remarkable for P&O strategy as seen in Figure 22. Results from static test shows that the mean and standard deviation for V_{ref} estimation of P&O are 9.99 V and 1.28, respectively. Whereas, the EA strategy presents 9.98 V and 0.14 V, respectively.

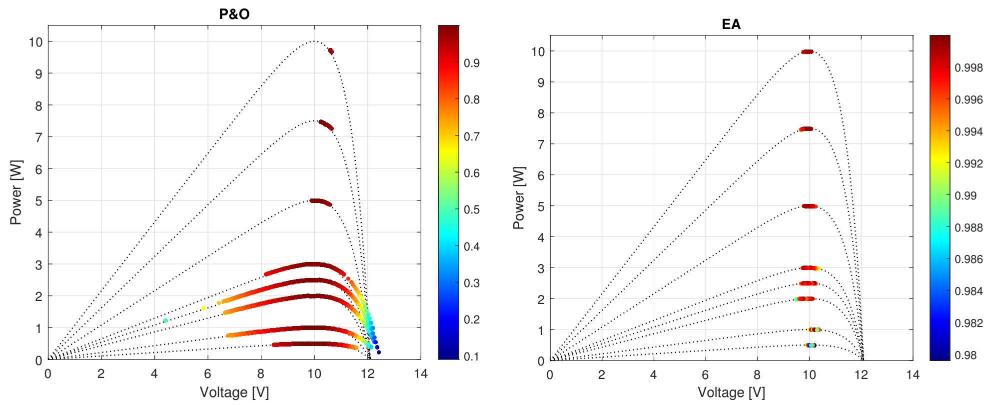

Figure 22. MPPTs behavior in static tests at V_{mp} = 10 V.

In the case of 12.5 V for MPP (Figure 23), the average and standard deviation for P&O are 12.70 V and 1.15 V. On the other hand, EA-V_{ref} strategy presents 12.32 V and 0.43 V, respectively. Likewise, the density plot depicts more steady-state oscillation for P&O strategy which is defined by the standard deviation aforementioned.

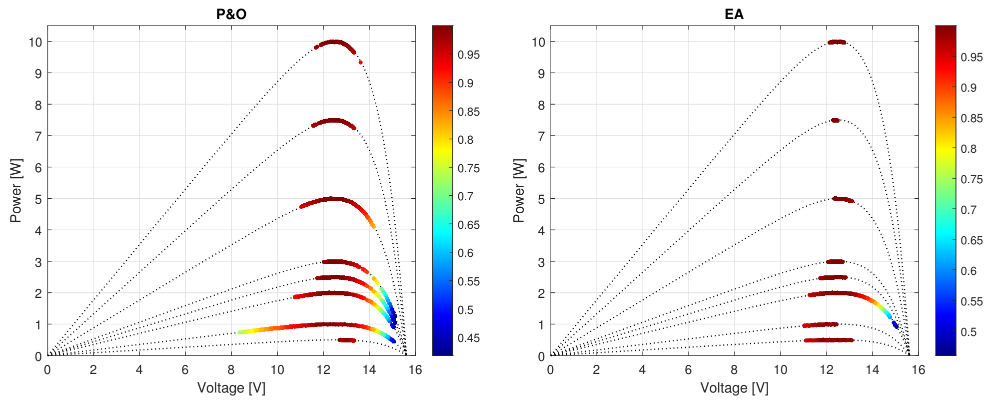

Figure 23. MPPTs behavior in static tests at V_{mp} = 12.5 V.

6.2. Dynamic Report

The dynamic test evaluates the tracking speed for MPP; in this case, V_{ref} is estimated by the MPPT algorithm and it is regulated by the PI controller which determined the correct duty cycle for the DC/DC converter. The results in Table 3 indicate that both MPPT-V_{ref} strategies present good performance and efficiency in dynamic responses. Hence, the MPPT tracking speed is well performed by the PI control loop and the FPGA implementation strategy.

Table 3. EN50530 dynamic test report.

Irradiance (W/m^2)	No. of Ramps	Duration (s)	P&O Efficiency (%)	EA Efficiency (%)
100–500	2	1940	99.905	99.592
	3	1560	99.884	99.520
	4	1447	99.895	99.824
	6	1380	99.892	99.685
	8	1374	99.857	99.627
	10	1300	99.427	99.630
	10	1071	99.129	99.589
	10	900	99.039	99.497
	10	767	98.755	99.282
	10	660	98.325	99.066
300–1000	10	1900	99.571	99.905
	10	1500	99.665	99.884
	10	1200	99.745	99.895
	10	967	99.809	99.892
	10	780	99.762	99.857
	10	640	99.677	99.427
10–100	1	2320	95.129	99.093

7. Conclusions

In this work, a new direct EA-MPPT strategy based on the EA metaheuristic optimization algorithm is used to estimate the optimal voltage to reach the V_{mp} of the PV system. Then, to reduce any error, a PI controller is integrated to rectify the optimal estimated EA-MPPT voltage, which is the V_{ref} for the PI controller that changes the duty cycle to achieve this voltage.

To compare and evaluate the performance, the counterpart (direct) method such as P&O-V_{ref} MPPT algorithm was implemented and tested because it is the most widely used for commercial products.

Moreover, a real PV system was experimentally characterized to reproduce the I-V and P-V curves into the NP8937APV Keysight® PV array simulator to evaluate the MPPT efficiency using the EN50530 standard test. This standard test was executed to evaluate the static and dynamic responses of both MPPT direct strategies in real-world weather condition from different regions.

In addition, these strategies were embedded on an FPGA (cRIO-9030) using LabVIEW as a programming language and FPGA module to deploy into the device. The main structure of FPGA implementation consisted of four parallel loops: (1) PWM generation signal, (2) signal conditioning and MPPT-$Vref$ estimation, (3) duty cycle estimation from PI controller, and (4) sending data for data collection through FIFOs.

Overall results show the feasibility of both MPPT-V_{ref} approach for LabVIEW FPGA hardware. Meanwhile, from static test results, EA-MPPT presented a better efficiency of 5.13% and 3.23% for European and CEC efficiency, respectively. Thus, EA-MPPT-V_{ref} reduces the steady-state oscillations when it is near of the MPP. On the other hand, dynamic test results showed that P&O strategy obtained an efficiency from 95.13% to 99.91%, while EA strategy captured from 99.01% to 99.91% of the total power of the PV system.

Author Contributions: Conceptualization and formal analysis, A.O., E.M. and I.M.; Software, A.O.; Investigation, A.O. and I.M.; Methodology, A.O., E.M. and I.M.; Project administration and resources, A.M.; Supervision, I.M. and A.M.; Validation, E.M. and I.M.; Writing—original draft, A.O.; Writing—review & editing, I.M. All authors have read and agreed to the published version of the manuscript.

Funding: We appreciate financial support through the Scholarships Program of CONACYT addressed to CVU 859994, Tecnologico de Monterrey.

Conflicts of Interest: The authors declare no conflict of interest.

Abbreviations

The following abbreviations are used in this manuscript:

ABC	Artificial bee colony
ACO	Ant colony optimization
ADC	Analog-to-digital converter
AI	Artificial intelligence
ANN	Artificial neural network
BA	Bat algorithm
CEC	California energy commission
cRIO	CompactRIO embedded controller
CS	Chaotic search
CSO	Cuckoo search optimization
DC	Direct current
DE	Differential evolution
dI	Incremental current
DO	Digital output
dV	Incremental voltage
EA	Earthquake optimization algorithm
FA	Firefly algorithm
FIFO	First-in, First-out
FL	Fuzzy-logic
FOCV	Fractional open-circuit voltage
FPGA	Field-programmable gate array
GA	Genetic algorithm
GWO	Grey wolf optimizer
I	Current
I_{mp}	Current at maximum power
IC	Incremental conductance
IEC	International electrotechnical commission
K_{pv}	Voltage factor constant
KF	Kalman-filter
MKE	Monkey king evolution
MPP	Maximum power point
MPPT	Maximum power point tracking
MPPT-V_{ref}	Reference voltage-based maximum power point tracking
P	Power
P&O	Perturb and observe
P_{mp}	Maximum power
PC	Personal computer
PI	proportional-integral controller
PSO	Particle swarm optimization
PVsim	Photovoltaic array simulator
PWM	pulse-width modulation
RMS	Root mean square
ROA	Remora optimization algorithm
S_{flag}	Searching flag
S_r	S-range
SAS	Solar array simulator
SCPI	Standard commands for programmable instruments
SFLA	Shuffled frog-leaping algorithm
SSA	Salp swarm algorithm
US	United states
V	Voltage

V_{mp}	Voltage at maximum power
V_{oc}	Open-circuit voltage
V_{pv}	Voltage of photovoltaic system
V_{ref}	Reference voltage
v_p	Velocity of P-wave
v_s	Velocity of S-wave
VISA	Virtual instrument software architecture

References

1. Kapilan, N.; Nithin, K.; Chiranth, K. Challenges and opportunities in solar photovoltaic system. *Mater. Today Proc.* **2022**, *62*, 3538–3543. [CrossRef]
2. Boghdady, T.A.; Kotb, Y.E.; Aljumah, A.; Sayed, M.M. Comparative Study of Optimal PV Array Configurations and MPPT under Partial Shading with Fast Dynamical Change of Hybrid Load. *Sustainability* **2022**, *14*, 2937. [CrossRef]
3. Lu, S.D.; Lin, C.H.; Huang, L.Y.; Lee, Y.L.; Liu, H.D.; Liao, P.C.; Gao, G.J.; Hsu, C.M. Novel Global-MPPT Control Strategy Considering the Variation in the Photovoltaic Module Output Power and Loads for Solar Power Systems. *Processes* **2022**, *10*, 367. [CrossRef]
4. Chao, K.H.; Chang, L.Y.; Wang, K.W. Global Maximum Power Point Tracking of Photovoltaic Module Arrays Based on Improved Cuckoo Search Algorithm. *Electronics* **2022**, *11*, 1247. [CrossRef]
5. Ahmed, M.; Harbi, I.; Kennel, R.; Rodríguez, J.; Abdelrahem, M. Maximum Power Point Tracking-Based Model Predictive Control for Photovoltaic Systems: Investigation and New Perspective. *Sensors* **2022**, *22*, 3069. [CrossRef] [PubMed]
6. Saravanan, D.; Singh, D.; Sinha, S.; Shaw, R.N.; Prabu, K. A Comprehensive Study of Well-Konown Maximum Power Point Tracking Techniques. In Proceedings of the 2020 IEEE International Conference on Computing, Power and Communication Technologies (GUCON), Greater Noida, India, 2–4 October 2020; pp. 829–837. [CrossRef]
7. Verma, D.; Nema, S.; Agrawal, R.; Sawle, Y.; Kumar, A. A Different Approach for Maximum Power Point Tracking (MPPT) Using Impedance Matching through Non-Isolated DC-DC Converters in Solar Photovoltaic Systems. *Electronics* **2022**, *11*, 1053. [CrossRef]
8. Andrejasic, T.; Jankovec, M.; Topic, M. Comparison of direct maximum power point tracking algorithms using EN 50530 dynamic test procedure. *IET Renew. Power Gener.* **2011**, *5*, 281–286. [CrossRef]
9. Bendib, B.; Belmili, H.; Krim, F. A survey of the most used MPPT methods: Conventional and advanced algorithms applied for photovoltaic systems. *Renew. Sustain. Energy Rev.* **2015**, *45*, 637–648. [CrossRef]
10. Dileep, G.; Singh, S. Application of soft computing techniques for maximum power point tracking of SPV system. *Sol. Energy* **2017**, *141*, 182–202. [CrossRef]
11. Motahhir, S.; El Hammoumi, A.; El Ghzizal, A. The most used MPPT algorithms: Review and the suitable low-cost embedded board for each algorithm. *J. Clean. Prod.* **2020**, *246*, 118983. . [CrossRef]
12. Femia, N.; Petrone, G.; Spagnuolo, G.; Vitelli, M. Optimization of perturb and observe maximum power point tracking method. *IEEE Trans. Power Electron.* **2005**, *20*, 963–973. [CrossRef]
13. Femia, N.; Granozio, D.; Petrone, G.; Spagnuolo, G.; Vitelli, M. Predictive & adaptive MPPT perturb and observe method. *IEEE Trans. Aerosp. Electron. Syst.* **2007**, *43*, 934–950.
14. Piegari, L.; Rizzo, R. Adaptive perturb and observe algorithm for photovoltaic maximum power point tracking. *IET Renew. Power Gener.* **2010**, *4*, 317–328. [CrossRef]
15. Sharma, D.; Purohit, G. Advanced perturbation and observation (P&O) based maximum power point tracking (MPPT) of a solar photo-voltaic system. In Proceedings of the 2012 IEEE 5th India International Conference on Power Electronics (IICPE), Delhi, India, 6–8 December 2012; pp. 1–5.
16. Jie, D.; Chun-jiang, Z.; Yan-bang, L. Comparison of duty ratio perturbation & observation and reference voltage perturbation & observation methods applied in MPPT. In Proceedings of the 7th International Power Electronics and Motion Control Conference, Harbin, China, 2–5 June 2012; Volume 2, pp. 1358–1362.
17. Sera, D.; Mathe, L.; Kerekes, T.; Spataru, S.V.; Teodorescu, R. On the perturb-and-observe and incremental conductance MPPT methods for PV systems. *IEEE J. Photovolt.* **2013**, *3*, 1070–1078. [CrossRef]
18. Ishaque, K.; Salam, Z.; Lauss, G. The performance of perturb and observe and incremental conductance maximum power point tracking method under dynamic weather conditions. *Appl. Energy* **2014**, *119*, 228–236. [CrossRef]
19. Harrag, A.; Messalti, S. Variable step size modified P&O MPPT algorithm using GA-based hybrid offline/online PID controller. *Renew. Sustain. Energy Rev.* **2015**, *49*, 1247–1260.
20. Verma, D.; Nema, S.; Nema, R. Implementation of perturb and observe method of maximum power point tracking in SIMSCAPE/MATLAB. In Proceedings of the 2017 International Conference on Intelligent Sustainable Systems (ICISS), Palladam, India, 7–8 December 2017; pp. 148–152.
21. Amarnath, R.; Verma, D. Harmonics Mitigation Of P&O MPPT Based Solar Powered Five-Level Diode-Clamped Multilevel Inverter. In Proceedings of the IEEE International Conference on Innovations in Control, Communication and Information System, Greater Noida, India, 12–13 August 2017.

22. Jain, K.; Gupta, M.; Bohre, A.K. Implementation and comparative analysis of P&O and INC MPPT method for PV system. In Proceedings of the 2018 8th IEEE India International Conference on Power Electronics (IICPE), Jaipur, India, 13–15 December 2018; pp. 1–6.
23. Liu, B.; Duan, S.; Liu, F.; Xu, P. Analysis and improvement of maximum power point tracking algorithm based on incremental conductance method for photovoltaic array. In Proceedings of the 2007 7th International Conference on Power Electronics and Drive Systems, Bangkok, Thailand, 27–30 November 2007; pp. 637–641.
24. Liu, F.; Duan, S.; Liu, F.; Liu, B.; Kang, Y. A Variable Step Size INC MPPT Method for PV Systems. *IEEE Trans. Ind. Electron.* **2008**, *55*, 2622–2628. [CrossRef]
25. Lin, C.H.; Huang, C.H.; Du, Y.C.; Chen, J.L. Maximum photovoltaic power tracking for the PV array using the fractional-order incremental conductance method. *Appl. Energy* **2011**, *88*, 4840–4847. [CrossRef]
26. Kumar, K.K.; Bhaskar, R.; Koti, H. Implementation of MPPT algorithm for solar photovoltaic cell by comparing short-circuit method and incremental conductance method. *Procedia Technol.* **2014**, *12*, 705–715. [CrossRef]
27. Tey, K.S.; Mekhilef, S. Modified incremental conductance MPPT algorithm to mitigate inaccurate responses under fast-changing solar irradiation level. *Sol. Energy* **2014**, *101*, 333–342. [CrossRef]
28. Radjai, T.; Rahmani, L.; Mekhilef, S.; Gaubert, J.P. Implementation of a modified incremental conductance MPPT algorithm with direct control based on a fuzzy duty cycle change estimator using dSPACE. *Sol. Energy* **2014**, *110*, 325–337. [CrossRef]
29. Sivakumar, P.; Kader, A.A.; Kaliavaradhan, Y.; Arutchelvi, M. Analysis and enhancement of PV efficiency with incremental conductance MPPT technique under non-linear loading conditions. *Renew. Energy* **2015**, *81*, 543–550. [CrossRef]
30. Hua, C.C.; Fang, Y.H.; Chen, W.T. Hybrid maximum power point tracking method with variable step size for photovoltaic systems. *IET Renew. Power Gener.* **2016**, *10*, 127–132. [CrossRef]
31. Baimel, D.; Tapuchi, S.; Levron, Y.; Belikov, J. Improved fractional open circuit voltage MPPT methods for PV systems. *Electronics* **2019**, *8*, 321. [CrossRef]
32. Mahmoud, A.; Mashaly, H.; Kandil, S.; El Khashab, H.; Nashed, M. Fuzzy logic implementation for photovoltaic maximum power tracking. In Proceedings of the 2000 26th Annual Conference of the IEEE Industrial Electronics Society. IECON 2000. 2000 IEEE International Conference on Industrial Electronics, Control and Instrumentation. 21st Century Technologies, Nagoya, Japan, 22–28 October 2000; Volume 1, pp. 735–740.
33. Veerachary, M.; Senjyu, T.; Uezato, K. Feedforward maximum power point tracking of PV systems using fuzzy controller. *IEEE Trans. Aerosp. Electron. Syst.* **2002**, *38*, 969–981. [CrossRef]
34. Khaehintung, N.; Pramotung, K.; Tuvirat, B.; Sirisuk, P. RISC-microcontroller built-in fuzzy logic controller of maximum power point tracking for solar-powered light-flasher applications. In Proceedings of the 30th Annual Conference of IEEE Industrial Electronics Society, 2004. IECON 2004, Busan, Korea, 2–6 November 2004; Volume 3, pp. 2673–2678.
35. Patcharaprakiti, N.; Premrudeepreechacharn, S.; Sriuthaisiriwong, Y. Maximum power point tracking using adaptive fuzzy logic control for grid-connected photovoltaic system. *Renew. Energy* **2005**, *30*, 1771–1788. [CrossRef]
36. Masoum, M.; Sarvi, M. Design, simulation and implementation of a fuzzybased maximum power point tracker under variable irradiance and temperature conditions. *Iran J. Sci. Technol.* **2005**, *29*, 27–32.
37. Kottas, T.L.; Boutalis, Y.S.; Karlis, A.D. New maximum power point tracker for PV arrays using fuzzy controller in close cooperation with fuzzy cognitive networks. *IEEE Trans. Energy Convers.* **2006**, *21*, 793–803. [CrossRef]
38. Varnham, A.; Al-Ibrahim, A.M.; Virk, G.S.; Azzi, D. Soft-computing model-based controllers for increased photovoltaic plant efficiencies. *IEEE Trans. Energy Convers.* **2007**, *22*, 873–880. [CrossRef]
39. Luo, W. The research of photovoltaic charging system based on fuzzy controller. In Proceedings of the 2009 Asia-Pacific Power and Energy Engineering Conference, Wuhan, China, 28–30 March 2009; pp. 1–4.
40. Syafaruddin; Karatepe, E.; Hiyama, T. Artificial neural network-polar coordinated fuzzy controller based maximum power point tracking control under partially shaded conditions. *IET Renew. Power Gener.* **2009**, *3*, 239–253. [CrossRef]
41. Chiu, C.S. TS fuzzy maximum power point tracking control of solar power generation systems. *IEEE Trans. Energy Convers.* **2010**, *25*, 1123–1132. [CrossRef]
42. Alajmi, B.N.; Ahmed, K.H.; Finney, S.J.; Williams, B.W. Fuzzy-logic-control approach of a modified hill-climbing method for maximum power point in microgrid standalone photovoltaic system. *IEEE Trans. Power Electron.* **2010**, *26*, 1022–1030. [CrossRef]
43. Messai, A.; Mellit, A.; Guessoum, A.; Kalogirou, S.A. Maximum power point tracking using a GA optimized fuzzy logic controller and its FPGA implementation. *Sol. Energy* **2011**, *85*, 265–277. [CrossRef]
44. Alabedin, A.Z.; El-Saadany, E.; Salama, M. Maximum power point tracking for Photovoltaic systems using fuzzy logic and artificial neural networks. In Proceedings of the 2011 IEEE Power and Energy Society General Meeting, Detroit, MI, USA, 24–28 July 2011; pp. 1–9.
45. Purnama, I.; Lo, Y.K.; Chiu, H.J. A fuzzy control maximum power point tracking photovoltaic system. In Proceedings of the 2011 IEEE International Conference on Fuzzy Systems (FUZZ-IEEE 2011), Taipei, Taiwan, 27–30 June 2011; pp. 2432–2439.
46. Algazar, M.M.; AL-monier, H.; Abd El-Halim, H.; Salem, M.E.E.K. Maximum power point tracking using fuzzy logic control. *Int. J. Electr. Power Energy Syst.* **2012**, *39*, 21–28. [CrossRef]
47. Othman, A.M.; El-arini, M.M.; Ghitas, A.; Fathy, A. Realworld maximum power point tracking simulation of PV system based on Fuzzy Logic control. *NRIAG J. Astron. Geophys.* **2012**, *1*, 186–194. [CrossRef]

48. Canny, D.; Yusivar, F. Maximum Power Point Tracking (MPPT) Algorithm Simulation Based on Fuzzy Logic Controller on Solar Cell with Boost Converter. In Proceedings of the 2018 2nd International Conference on Smart Grid and Smart Cities (ICSGSC), Kuala Lumpur, Malaysia, 12–14 August 2018; pp. 117–121. [CrossRef]
49. Harrag, A.; Messalti, S. IC-based Variable Step Size Neuro-Fuzzy MPPT Improving PV System Performances. *Energy Procedia* **2019**, *157*, 362–374. [CrossRef]
50. Rezk, H.; Aly, M.; Al-Dhaifallah, M.; Shoyama, M. Design and Hardware Implementation of New Adaptive Fuzzy Logic-Based MPPT Control Method for Photovoltaic Applications. *IEEE Access* **2019**, *7*, 106427–106438. [CrossRef]
51. Ge, X.; Ahmed, F.W.; Rezvani, A.; Aljojo, N.; Samad, S.; Foong, L.K. Implementation of a novel hybrid BAT-Fuzzy controller based MPPT for grid-connected PV-battery system. *Control Eng. Pract.* **2020**, *98*, 104380. [CrossRef]
52. Ocran, T.A.; Cao, J.; Cao, B.; Sun, X. Artificial neural network maximum power point tracker for solar electric vehicle. *Tsinghua Sci. Technol.* **2005**, *10*, 204–208. [CrossRef]
53. Lin, W.M.; Hong, C.M.; Chen, C.H. Neural-Network-Based MPPT Control of a Stand-Alone Hybrid Power Generation System. *IEEE Trans. Power Electron.* **2011**, *26*, 3571–3581. [CrossRef]
54. Asiful Islam, M.; Ashfanoor Kabir, M. Neural network based maximum power point tracking of photovoltaic arrays. In Proceedings of the TENCON 2011—2011 IEEE Region 10 Conference, Bali, Indonesia, 21–24 November 2011; pp. 79–82. [CrossRef]
55. Jie, L.; Ziran, C. Research on the MPPT algorithms of photovoltaic system based on PV neural network. In Proceedings of the 2011 Chinese Control and Decision Conference (CCDC), Mianyang, China, 23–25 May 2011; pp. 1851–1854.
56. Subiyanto, S.; Mohamed, A.; Hannan, M. Intelligent maximum power point tracking for PV system using Hopfield neural network optimized fuzzy logic controller. *Energy Build.* **2012**, *51*, 29–38. [CrossRef]
57. Liu, Y.H.; Liu, C.L.; Huang, J.W.; Chen, J.H. Neural-network-based maximum power point tracking methods for photovoltaic systems operating under fast changing environments. *Sol. Energy* **2013**, *89*, 42–53. [CrossRef]
58. Punitha, K.; Devaraj, D.; Sakthivel, S. Artificial neural network based modified incremental conductance algorithm for maximum power point tracking in photovoltaic system under partial shading conditions. *Energy* **2013**, *62*, 330–340. [CrossRef]
59. Sahnoun, M.A.; Ugalde, H.M.R.; Carmona, J.C.; Gomand, J. Maximum Power point Tracking Using P&O Control Optimized by a Neural Network Approach: A Good Compromise between Accuracy and Complexity. *Energy Procedia* **2013**, *42*, 650–659. [CrossRef]
60. Seyedmahmoudian, M.; Horan, B.; Soon, T.K.; Rahmani, R.; Than Oo, A.M.; Mekhilef, S.; Stojcevski, A. State of the art artificial intelligence-based MPPT techniques for mitigating partial shading effects on PV systems—A review. *Renew. Sustain. Energy Rev.* **2016**, *64*, 435–455. [CrossRef]
61. Verma, D.; Nema, S.; Shandilya, A.; Dash, S.K. Maximum power point tracking (MPPT) techniques: Recapitulation in solar photovoltaic systems. *Renew. Sustain. Energy Rev.* **2016**, *54*, 1018–1034. [CrossRef]
62. Kumar P.K., V.; Manjunath, K. A Comparitive Analysis of MPPT Algorithms for Solar Photovoltaic Systems to Improve the Tracking Accuracy. In Proceedings of the 2018 International Conference on Control, Power, Communication and Computing Technologies (ICCPCCT), Kannur, India, 23–24 March 2018; pp. 540–547. [CrossRef]
63. Al-Wesabi, I.; Fang, Z.; Farh, H.M.H.; Al-Shamma'a, A.A.; Al-Shaalan, A.M.; Kandil, T.; Ding, M. Cuckoo Search Combined with PID Controller for Maximum Power Extraction of Partially Shaded Photovoltaic System. *Energies* **2022**, *15*, 2513. [CrossRef]
64. Banakhr, F.A.; Mosaad, M.I. High performance adaptive maximum power point tracking technique for off-grid photovoltaic systems. *Sci. Rep.* **2021**, *11*,20400. [CrossRef]
65. Cruz, P.P.; Gutiérrez, A.M.; Ramírez-Mendoza, R.A.; Flores, E.M.; Espinoza, A.A.O.; Silva, D.C.B. *A Practical Approach to Metaheuristics Using LabVIEW and MATLAB®*; Chapman and Hall/CRC: Boca Raton, FL, USA, 2020.
66. Torres-Jiménez, J.; Pavón, J. Applications of metaheuristics in real-life problems. *Prog. Artif. Intell.* **2014**, *2*, 175–176. [CrossRef]
67. Alanazi, A.; Alanazi, M.; Arabi, S.; Sarker, S. A New Maximum Power Point Tracking Framework for Photovoltaic Energy Systems Based on Remora Optimization Algorithm in Partial Shading Conditions. *Appl. Sci.* **2022**, *12*, 3828. [CrossRef]
68. Kuo, J.L.; Chao, K.L.; Lee, L.S. Dual Mechatronic MPPT Controllers With PN and OPSO Control Algorithms for the Rotatable Solar Panel in PHEV System. *IEEE Trans. Ind. Electron.* **2010**, *57*, 678–689. [CrossRef]
69. Miyatake, M.; Veerachary, M.; Toriumi, F.; Fujii, N.; Ko, H. Maximum Power Point Tracking of Multiple Photovoltaic Arrays: A PSO Approach. *IEEE Trans. Aerosp. Electron. Syst.* **2011**, *47*, 367–380. [CrossRef]
70. Fu, Q.; Tong, N. A new fuzzy control method based on PSO for Maximum Power Point Tracking of photovoltaic system. In Proceedings of the 2011 International Conference on Computer Science and Network Technology, Harbin, China, 24–26 December 2011; Volume 3, pp. 1487–1491. [CrossRef]
71. Liu, Y.H.; Huang, S.C.; Huang, J.W.; Liang, W.C. A Particle Swarm Optimization-Based Maximum Power Point Tracking Algorithm for PV Systems Operating Under Partially Shaded Conditions. *IEEE Trans. Energy Convers.* **2012**, *27*, 1027–1035. [CrossRef]
72. Ishaque, K.; Salam, Z.; Shamsudin, A.; Amjad, M. A direct control based maximum power point tracking method for photovoltaic system under partial shading conditions using particle swarm optimization algorithm. *Appl. Energy* **2012**, *99*, 414–422. [CrossRef]
73. Ishaque, K.; Salam, Z.; Amjad, M.; Mekhilef, S. An improved particle swarm optimization (PSO)–based MPPT for PV with reduced steady-state oscillation. *IEEE Trans. Power Electron.* **2012**, *27*, 3627–3638. [CrossRef]
74. Ishaque, K.; Salam, Z. A Deterministic Particle Swarm Optimization Maximum Power Point Tracker for Photovoltaic System Under Partial Shading Condition. *IEEE Trans. Ind. Electron.* **2013**, *60*, 3195–3206. [CrossRef]

75. Seyedmahmoudian, M.; Rahmani, R.; Mekhilef, S.; Maung Than Oo, A.; Stojcevski, A.; Soon, T.K.; Ghandhari, A.S. Simulation and Hardware Implementation of New Maximum Power Point Tracking Technique for Partially Shaded PV System Using Hybrid DEPSO Method. *IEEE Trans. Sustain. Energy* **2015**, *6*, 850–862. [CrossRef]
76. Shi, J.; Zhang, W.; Zhang, Y.; Xue, F.; Yang, T. MPPT for PV systems based on a dormant PSO algorithm. *Electr. Power Syst. Res.* **2015**, *123*, 100–107. [CrossRef]
77. Pragallapati, N.; Sen, T.; Agarwal, V. Adaptive Velocity PSO for Global Maximum Power Control of a PV Array Under Nonuniform Irradiation Conditions. *IEEE J. Photovolt.* **2017**, *7*, 624–639. [CrossRef]
78. Ramaprabha, R.; Mathur, B. Intelligent controller based maximum power point tracking for solar PV system. *Int. J. Comput. Appl.* **2011**, *12*, 37–41. [CrossRef]
79. Daraban, S.; Petreus, D.; Morel, C. A novel MPPT (maximum power point tracking) algorithm based on a modified genetic algorithm specialized on tracking the global maximum power point in photovoltaic systems affected by partial shading. *Energy* **2014**, *74*, 374–388. [CrossRef]
80. Rezvani, A.; Izadbakhsh, M.; Gandomkar, M.; Vafaei, S. Investigation of ANN-GA and modified perturb and observe MPPT techniques for photovoltaic system in the grid connected mode. *Indian J. Sci. Technol.* **2015**, *8*, 87. [CrossRef]
81. Kumar, P.; Jain, G.; Palwalia, D.K. Genetic algorithm based maximum power tracking in solar power generation. In Proceedings of the 2015 International Conference on Power and Advanced Control Engineering (ICPACE), Bengaluru, India, 12–14 August 2015; pp. 1–6. [CrossRef]
82. Badis, A.; Mansouri, M.N.; Sakly, A. PSO and GA-based maximum power point tracking for partially shaded photovoltaic systems. In Proceedings of the 2016 7th International Renewable Energy Congress (IREC), Hammamet, Tunisia, 22–24 March 2016; pp. 1–6. [CrossRef]
83. Taheri, H.; Salam, Z.; Ishaque, K.; Syafaruddin. A novel Maximum Power Point tracking control of photovoltaic system under partial and rapidly fluctuating shadow conditions using Differential Evolution. In Proceedings of the 2010 IEEE Symposium on Industrial Electronics and Applications (ISIEA), Penang, Malaysia, 3–5 October 2010; pp. 82–87. [CrossRef]
84. Joisher, M.; Singh, D.; Taheri, S.; Espinoza-Trejo, D.R.; Pouresmaeil, E.; Taheri, H. A hybrid evolutionary-based MPPT for photovoltaic systems under partial shading conditions. *IEEE Access* **2020**, *8*, 38481–38492. [CrossRef]
85. Ahmed, J.; Salam, Z. A soft computing MPPT for PV system based on Cuckoo Search algorithm. In Proceedings of the 4th International Conference on Power Engineering, Energy and Electrical Drives, Istanbul, Turkey, 13–17 May 2013; pp. 558–562. [CrossRef]
86. Nugraha, D.A.; Lian, K.L.; Suwarno. A Novel MPPT Method Based on Cuckoo Search Algorithm and Golden Section Search Algorithm for Partially Shaded PV System. *Can. J. Electr. Comput. Eng.* **2019**, *42*, 173–182. [CrossRef]
87. Adly, M.; Besheer, A. An optimized fuzzy maximum power point tracker for stand alone photovoltaic systems: Ant colony approach. In Proceedings of the 2012 7th IEEE Conference on Industrial Electronics and Applications (ICIEA), Singapore, 18–20 July 2012; pp. 113–119. [CrossRef]
88. Jiang, L.L.; Maskell, D.L.; Patra, J.C. A novel ant colony optimization-based maximum power point tracking for photovoltaic systems under partially shaded conditions. *Energy Build.* **2013**, *58*, 227–236. . [CrossRef]
89. Titri, S.; Larbes, C.; Toumi, K.Y.; Benatchba, K. A new MPPT controller based on the Ant colony optimization algorithm for Photovoltaic systems under partial shading conditions. *Appl. Soft Comput.* **2017**, *58*, 465–479. [CrossRef]
90. Sundareswaran, K.; Peddapati, S.; Palani, S. MPPT of PV Systems Under Partial Shaded Conditions Through a Colony of Flashing Fireflies. *IEEE Trans. Energy Convers.* **2014**, *29*, 463–472. [CrossRef]
91. Teshome, D.F.; Lee, C.H.; Lin, Y.W.; Lian, K.L. A Modified Firefly Algorithm for Photovoltaic Maximum Power Point Tracking Control Under Partial Shading. *IEEE J. Emerg. Sel. Top. Power Electron.* **2017**, *5*, 661–671. [CrossRef]
92. Zhou, L.; Chen, Y.; Guo, K.; Jia, F. New Approach for MPPT Control of Photovoltaic System With Mutative-Scale Dual-Carrier Chaotic Search. *IEEE Trans. Power Electron.* **2011**, *26*, 1038–1048. [CrossRef]
93. Oshaba, A.; Ali, E.; Abd Elazim, S. Artificial bee colony algorithm based maximum power point tracking in photovoltaic system. *WSEAS Trans. Power Syst* **2015**, *10*, 22.
94. Mohanty, S.; Subudhi, B.; Ray, P.K. A New MPPT Design Using Grey Wolf Optimization Technique for Photovoltaic System Under Partial Shading Conditions. *IEEE Trans. Sustain. Energy* **2016**, *7*, 181–188. [CrossRef]
95. Kaced, K.; Larbes, C.; Ramzan, N.; Bounabi, M.; elabadine Dahmane, Z. Bat algorithm based maximum power point tracking for photovoltaic system under partial shading conditions. *Sol. Energy* **2017**, *158*, 490–503. [CrossRef]
96. Sridhar, R.; Jeevananthan, S.; Dash, S.S.; Vishnuram, P. A new maximum power tracking in PV system during partially shaded conditions based on shuffled frog leap algorithm. *J. Exp. Theor. Artif. Intell.* **2017**, *29*, 481–493. [CrossRef]
97. Kumar, N.; Hussain, I.; Singh, B.; Panigrahi, B.K. Maximum power peak detection of partially shaded PV panel by using intelligent monkey king evolution algorithm. In Proceedings of the 2016 IEEE International Conference on Power Electronics, Drives and Energy Systems (PEDES), Trivandrum, India, 14–17 December 2016; pp. 1–6. [CrossRef]
98. Yang, B.; Zhong, L.; Zhang, X.; Shu, H.; Yu, T.; Li, H.; Jiang, L.; Sun, L. Novel bio-inspired memetic salp swarm algorithm and application to MPPT for PV systems considering partial shading condition. *J. Clean. Prod.* **2019**, *215*, 1203–1222. [CrossRef]
99. Mendez, E.; Ortiz, A.; Ponce, P.; Macias, I.; Balderas, D.; Molina, A. Improved MPPT algorithm for photovoltaic systems based on the earthquake optimization algorithm. *Energies* **2020**, *13*, 3047. [CrossRef]

100. Mendez, E.; Ortiz, A.; Ponce, P.; Acosta, J.; Molina, A. Mobile phone usage detection by ann trained with a metaheuristic algorithm. *Sensors* **2019**, *19*, 3110. [CrossRef]
101. Zhang, L.; Sun, K.; Hu, H.; Xing, Y. A System-Level Control Strategy of Photovoltaic Grid-Tied Generation Systems for European Efficiency Enhancement. *IEEE Trans. Power Electron.* **2014**, *29*, 3445–3453. [CrossRef]
102. Kalathil, A.; Krishnamurthy, H. Quantification of solar inverter efficiency for Indian tropical climatic conditions. In Proceedings of the 2014 IEEE Region 10 Humanitarian Technology Conference (R10 HTC), Chennai, India, 6–9 August 2014; pp. 14–18. [CrossRef]
103. Abdelsalam, A.K.; Massoud, A.M.; Ahmed, S.; Enjeti, P.N. High-Performance Adaptive Perturb and Observe MPPT Technique for Photovoltaic-Based Microgrids. *IEEE Trans. Power Electron.* **2011**, *26*, 1010–1021. [CrossRef]
104. Eltawil, M.A.; Zhao, Z. MPPT techniques for photovoltaic applications. *Renew. Sustain. Energy Rev.* **2013**, *25*, 793–813. [CrossRef]
105. Villalva, M.G.; Ruppert F., E. Analysis and simulation of the P&O MPPT algorithm using a linearized PV array model. In Proceedings of the 2009 35th Annual Conference of IEEE Industrial Electronics, Porto, Portugal, 3–5 November 2009; pp. 231–236. [CrossRef]
106. Femia, N.; Petrone, G.; Spagnuolo, G.; Vitelli, M. Optimizing sampling rate of P&O MPPT technique. In Proceedings of the 2004 IEEE 35th Annual Power Electronics Specialists Conference (IEEE Cat. No.04CH37551), Aachen, Germany, 20–25 June 2004; Volume 3, pp. 1945–1949. [CrossRef]
107. Rezoug, M.R.; Chenni, R.; Taibi, D. Fuzzy Logic-Based Perturb and Observe Algorithm with Variable Step of a Reference Voltage for Solar Permanent Magnet Synchronous Motor Drive System Fed by Direct-Connected Photovoltaic Array. *Energies* **2018**, *11*, 462. [CrossRef]
108. Ortiz, A.; Mendez, E.; Balderas, D.; Ponce, P.; Macias, I.; Molina, A. Hardware implementation of metaheuristics through LabVIEW FPGA. *Appl. Soft Comput.* **2021**, *113*, 107908. [CrossRef]
109. Ortiz, A.; Molina, A.; Macias, I.; Ramirez, M. Plataforma Integral para el Analisis Fuera de Linea de Patrones de Consumo Electrico en Sistemas Distribuidos de Energia. MX Request Patent MXa/2019/00700, 2019.
110. Technologies, K. Keysight N8900 Series Autoranging System DC Power Supply. 2019. Available online: https://www.keysight.com/us/en/support/N8937APV/photovoltaic-array-simulator-1500vdc-208vac.html (accessed on 1 October 2022).
111. Mendez, E.; Macias, I.; Ortiz, A.; Ponce, P.; Vargas-Martinez, A.; Lozoya-Santos, J.d.J.; Ramirez-Mendoza, R.A.; Morales-Menendez, R.; Molina, A. Novel design methodology for DC-DC converters applying metaheuristic optimization for inductance selection. *Appl. Sci.* **2020**, *10*, 4377. [CrossRef]